In Vivo Evaluation of ^{11}C-Preladenant for PET Imaging of Adenosine A_{2A} Receptors in the Conscious Monkey

Xiaoyun Zhou[1], Ronald Boellaard[1], Kiichi Ishiwata[2–4], Muneyuki Sakata[2], Rudi A.J.O. Dierckx[1], Johan R. de Jong[1], Shingo Nishiyama[5], Hiroyuki Ohba[5], Hideo Tsukada[5], Erik F.J. de Vries[1], and Philip H. Elsinga[1]

[1]University of Groningen, University Medical Center Groningen, Groningen, The Netherlands; [2]Research Team for Neuroimaging, Tokyo Metropolitan Institute of Gerontology, Tokyo, Japan; [3]Institute of Cyclotron and Drug Discovery Research, Southern TOHOKU Research Institute for Neuroscience, Koriyama, Japan; [4]Department of Biofunctional Imaging, Fukushima Medical University, Fukushima, Japan; and [5]Central Research Laboratory, Hamamatsu Photonics K.K., Hamamatsu, Japan

^{11}C-preladenant was developed as a novel PET ligand for the adenosine A_{2A} receptors (A_{2A}Rs). The present study aimed to evaluate the suitability of ^{11}C-preladenant PET for the quantification of striatal A_{2A}Rs and the assessment of A_{2A}R occupancy in the conscious monkey brain. **Methods:** ^{11}C-preladenant was intravenously injected into conscious monkeys (n = 4, 18 PET scans), and a 91-min dynamic scan was started. Arterial blood samples in combination with metabolite analysis were obtained during the scan to provide the input function for kinetic modeling. The distribution volume (V_T) was obtained by kinetic modeling with a 2-tissue-compartment model. The simplified reference tissue model (SRTM) with selected reference regions (cerebellum, cingulate, parietal cortex, and occipital cortex) was tested to estimate the binding potential (BP_{ND}) in A_{2A}R-rich regions. BP_{ND} obtained from the SRTM was compared with distribution volume ratio (DVR)-1. The effects of blood volume, blood delay, and scan duration on BP_{ND} and DVR-1 were investigated. V_T and BP_{ND} were also obtained after preblocking with unlabeled preladenant (1 mg/kg), A_{2A}R-selective KW-6002 (0.5–1 mg/kg), and nonselective adenosine receptor antagonist caffeine (2.5–10 mg/kg). A_{2A}R occupancy was studied with caffeine blockade. **Results:** Regional uptake of ^{11}C-preladenant was consistent with the distribution of A_{2A}Rs in the monkey brain, with the highest uptake in the putamen, followed by the caudate, and the lowest uptake in the cerebellum. Tracer kinetics were well described by the 2-tissue-compartment model with a lower constraint on k_4 to stabilize fits. The highest V_T was observed in A_{2A}R-rich regions (~5.8–7.4) and lowest value in the cerebellum (~1.3). BP_{ND} values estimated from the SRTM with different scan durations were comparable and were in agreement with DVR-1 (~4.3–5.3 in A_{2A}R-rich regions). Preladenant preinjection decreased the tracer uptake in A_{2A}R-rich regions to the level of the reference regions. Caffeine pretreatment reduced the tracer uptake in the striatum in a dose-dependent manner. **Conclusion:** ^{11}C-preladenant PET is suitable for noninvasive quantification of A_{2A}Rs and assessment of A_{2A}R occupancy in A_{2A}R-rich regions in the monkey brain. SRTM using the cerebellum as the reference tissue is the applicable model for A_{2A}R quantification.

Key Words: adenosine A_{2A} receptors; PET; ^{11}C-preladenant; pharmacokinetic modeling; monkey

J Nucl Med 2017; 58:762–767
DOI: 10.2967/jnumed.116.182410

The adenosine A_{2A} receptor (A_{2A}R) has drawn much attention in the past decades, because it has been implicated in brain disorders such as depression (*1*), Huntington disease (*2*), Alzheimer disease (*3*), and Parkinson disease (*4*). Consequently, the A_{2A}R has been studied as a potential target for central nervous system disorders, and several A_{2A}R antagonists were tested in clinical trials as antiparkinsonism drugs (*5*).

PET with a suitable A_{2A}R radioligand provides a unique opportunity to study A_{2A}R availability and function in vivo. This is exemplified by the in vivo imaging studies of the Parkinson brain with A_{2A}R radioligands ^{11}C-SCH442416 (*6*) and ^{11}C-TMSX (*7*). In addition, A_{2A}R availability was assessed with ^{11}C-TMSX in secondary progressive multiple sclerosis (*8*). Differences were found in the striatum between the drug-naïve and levodopa-treated Parkinson patients and in normal-appearing white matter between secondary progressive multiple sclerosis patients and healthy volunteers. However, because of the unfavorable properties of the radioligands, such as low target-to-nontarget ratio and high uptake in brain regions with negligible levels of A_{2A}Rs (*6,7,9*), the results were difficult to interpret, and therefore the usefulness of PET imaging with A_{2A}R radioligands is still to be proven.

We have recently synthesized ^{11}C-preladenant (*10*), an A_{2A}R antagonist with high affinity (k_i = 1.1 nM for human A_{2A}R) and selectivity toward A_{2A}R (*11*). PET imaging in rats showed a high uptake of ^{11}C-preladenant in the striatum and low uptake in extrastriatal regions, which was in agreement with cerebral A_{2A}R distribution (*10,12*).

On the basis of the encouraging results from the rodent studies, here we further evaluated ^{11}C-preladenant in conscious monkeys, as such a procedure rules out the possible effects of anesthesia on the kinetics of the tracer and A_{2A}R ligands. We characterized the pharmacokinetic properties of the tracer with kinetic modeling. Furthermore, we studied the striatal A_{2A}R occupancy by the nonselective adenosine receptor antagonist caffeine, the most studied A_{2A}R antagonist. This study serves as a prelude toward first-in-human PET studies.

Received Aug. 10, 2016; revision accepted Nov. 10, 2016.
For correspondence or reprints contact: Philip H. Elsinga, Nuclear Medicine and Molecular Imaging, University Medical Center Groningen, University of Groningen, Hanzeplein 1, 9713GZ Groningen, The Netherlands.
E-mail: p.h.elsinga@umcg.nl
Published online Jan. 6, 2017.

MATERIALS AND METHODS

Synthesis of ^{11}C-Preladenant

^{11}C-preladenant was prepared according to the procedure described by Zhou et al. (*10*) with some modifications. The final product was obtained in a practical yield of 2.78 ± 1.32 GBq, with a radiochemical purity of 98.2% ± 1.5% and a specific activity of 28.1 ± 10.9 GBq/μmol at the time of injection.

Animals

Animals were maintained and handled in accordance with the recommendations of the U.S. National Institutes of Health and the guidelines of the Central Research Laboratory, Hamamatsu Photonics. All experiments were approved by the Ethical Committee of the Central Research Laboratory, Hamamatsu Photonics (HPK-2014-12). Four young male rhesus monkeys (*Macaca mulatta*, 5.0–8.5 kg) were used for the PET measurements (baseline, $n = 7$; pretreatment with caffeine [Sigma], $n = 3$; pretreatment with 1 mg/kg preladenant [Chemscene, LLC], $n = 3$; pretreatment with 0.5 mg/kg KW-6002 [Axon Medchem BV], $n = 4$ [2 without blood sampling]; pretreatment with 1 mg/kg KW-6002, $n = 1$) in a conscious state. Each blocker was intravenously injected 30 min before injection of ^{11}C-preladenant. T1-weighted MR images of the monkeys were obtained with a 3.0-T MR imager (Signa sExcite HDxt 3.0 T; GE Healthcare Japan). MR images were reconstructed into a 256 × 256 × 178 matrix, with a voxel size of 0.4 × 0.4 × 0.7 mm.

PET Measurements

After overnight fasting, a venous cannula for PET ligand or blocker injection was inserted in one inferior limb and an arterial cannula for blood sampling was inserted in the other inferior limb. The PET scan was obtained using an animal PET scanner (SHR-7700; Hamamatsu Photonics) (*13*). After a transmission scan using a [^{68}Ge]-[^{68}Ga] rotation rod source, a 91-min dynamic acquisition was started at the time of ^{11}C-preladenant (~1 GBq) injection. Arterial blood samples were obtained manually over the acquisition. Blood and plasma were separated by centrifugation. The radioactivity in blood and plasma samples was measured using a well-counter (1480 WIZARD; Perkin Elmer). The percentage of radioactivity consisting of intact tracer in plasma was determined by radio–thin-layer chromatography with a mobile phase of chloroform/methanol (9/1, v/v).

PET Data Analysis

Dynamic PET data were histogrammed into 49 frames (6 × 10, 6 × 30, 12 × 60, and 25 × 180 s). The frames were reconstructed by filtered backprojection with a Hanning filter of 4.5 mm in full width at half maximum and corrected for attenuation, scatter, and random coincidences. All images contained 100 × 100 × 20 voxels with a voxel size of 1.2 × 1.2 × 3.6 mm. Individual PET and MR images were coregistered. Volumes of interest were drawn manually on the individual MR images, using regional information from BrainMaps.org (*14*) as an anatomic reference. MR image–derived volumes of interest were superimposed on the coregistered PET images to extract time–activity curves for kinetic analysis. Time–activity curves were normalized to body weight and injected activity to yield SUVs.

Tracer Kinetic Modeling

Tracer kinetics were quantified with PMOD software (version 3.5; PMOD Technologies). The fractional blood volume (V_B) in the brain was either fixed to 0%, 3%, or 5% or used as a fit parameter to assess the effect of blood volume on kinetic parameters. The blood delay was either fixed to 0 or used as a fit parameter. In addition, to stabilize kinetic model fits we explored both fitting or fixing k_4 for several reference regions (i.e., regions showing no or minimal specific binding). In the case of fixing, k_4 was set to 0, 0.005, 0.011, 0.02, or 0.04 min^{-1}.

A monoexponential function was fitted to the intact tracer fraction over time. A standard 2-parameter (K_1, k_2) 1-TCM (1-tissue-compartment model) and a 4-parameter (K_1, K_1/k_2, k_3, k_4) 2-TCM (2-tissue-compartment model) with and without V_B using a metabolite-corrected plasma input function were used to fit time–activity curves. The effects of variation in V_B, blood delay, reference region, k_4, and scan duration on model fits were judged by Akaike information criterion (AIC) and by the observed kinetic parameters (i.e., V_T, nondisplaceable distribution volume [V_{ND}], DVR-1, and BP_{ND}). BP_{ND} in the striatum was obtained by DVR-1 ($= V_T/V_{ND} - 1$) (*15*) as well as SRTM (Supplemental Fig. 1; supplemental materials are available at http://jnm.snmjournals.org). The invasive- and noninvasive model–derived BP_{ND} values were compared, using DVR-1 with a full scan length of 91 min as the gold standard. The cerebellum, cingulate, parietal cortex, and occipital cortex were tested as reference regions. The striatum was used as the target region in all data analyses. The test–retest variability (TRV) was compared between models and reference regions. TRV was calculated as $\text{TRV} = 2 \times |BP_{ND,\ test} - BP_{ND,\ retest}|/(BP_{ND,\ test} + BP_{ND,\ retest})$ or $\text{TRV} = 2 \times |V_{T,\ test} - V_{T,\ retest}|/(V_{T,\ test} + V_{T,\ retest})$.

A_{2A}R Occupancy by Caffeine

Three PET scans after administration of 2.5, 5, and 10 mg/kg of caffeine were obtained as described above, whereas blood sampling was acquired only for the caffeine dose of 2.5 mg/kg because of logistical reasons. Receptor occupancy was calculated from SRTM-derived BP_{ND} as $\text{occupancy} = \frac{BP_{ND,\ baseline} - BP_{ND,\ blocking}}{BP_{ND,\ baseline}} \times 100\%$, where the $BP_{ND,\ baseline}$ was obtained by averaging test and retest BP_{ND} at baseline of individual animals.

Statistics

The Wilcoxon signed-rank test was used to assess the difference in plasma activity and intact tracer fraction between baseline and A_{2A}R-blocker pretreatment, the effects of A_{2A}R-blocker pretreatment on V_T, and the difference in AIC between 1-TCM and 2-TCM. A Bland–Altman plot (difference [Δ] vs. mean) was used to judge the agreement between BP_{ND} and DVR-1. Δ (%) was computed as $\Delta = 2 \times 100 \times (BP_{ND} - [\text{DVR-1}])/(BP_{ND} + [\text{DVR-1}])$. A probability value of P less than 0.05 was considered to be statistically significant.

RESULTS

Kinetics of ^{11}C-Preladenant in Plasma

Figure 1 shows the plasma kinetics and metabolic radioactivity profile of ^{11}C-preladenant during the 91-min scan. KW-6002 and preladenant pretreatment did not significantly alter tracer metabolic rate (Fig. 1B) but caused significantly higher ($P < 0.05$) plasma radioactive levels between 24 and 40 s after injection than at baseline (Fig. 1A). The tracer metabolic pattern could be fitted with a monoexponential function with 32% ± 7% of radioactivity in plasma consisting of intact tracer at 90 min after injection. The metabolite-corrected plasma curve at baseline was well described with a biexponential function, with a distributive half-life of 0.15 ± 0.03 min and an elimination half-life of 6.86 ± 2.19 min.

Tracer Kinetic Modeling

The 2-TCM fitted the data better than the 1-TCM, with significantly ($P < 0.001$) lower (~2%–19%) AIC values for all volumes of interest and visually better agreement between the fitted curves and the experimental data (for clarity, only 2-TCM fits are shown in Fig. 2A). Therefore, the 2-TCM was used to quantify tracer kinetics. Variation in the V_B, blood delay, and k_4 value in reference regions did not substantially affect AIC values, because only a 0%–9% difference was found between various fits.

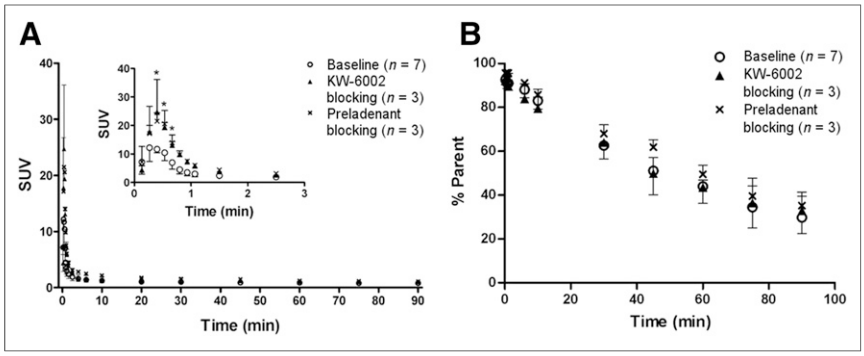

FIGURE 1. Kinetics of ^{11}C-preladenant in monkey plasma. (A) Time course of total activity in plasma at baseline and after blocker pretreatment. Insert shows first 3 min of plasma kinetics. (B) Parent fraction in plasma at baseline and after blocker pretreatment. Error bars indicate SD. $^{*}P < 0.05$.

Still, best fits (smaller AIC) were obtained when V_B was either fixed to 5% or included as a fit parameter, blood delay was included as a fit parameter, and the reference region k_4 was either fixed to 0.011 min^{-1} or included as a fit parameter.

The V_{ND} was estimated from the V_T of a reference region (i.e., cerebellum) at baseline and a target region (i.e., striatum) with $A_{2A}R$ binding sites completely blocked with preladenant. The effect of different V_B and k_4 values on estimated V_{ND} was analyzed. The V_B had little effect on either V_{ND} or V_T because a less than 10% difference was found with various V_B values. The effect of k_4 on V_{ND} is shown in Figure 3. The range of fit values for k_4 was chosen on the basis of an average cerebellar k_4 value of 0.011 min^{-1} (17% coefficient of variation [COV]) estimated by 2-TCM from 5 of 7 baseline scans. The excluded 2 cases provided low estimates on k_4 (0.0031 and 0.0056 min^{-1}), resulting in upward-biased V_{ND} values of 3.1 and 2.6, respectively, which were considered outliers (Supplemental Fig. 2). Indeed, when k_4 was small (0.005 min^{-1}) or without constraint, V_{ND} seemed to be overestimated in 1 or 2 cases at baseline. 2-TCM with k_4 between 0.011 and 0.04 min^{-1} estimated V_{ND} values within an acceptable range (i.e., $0 < V_{ND} < 2$), whereas larger fixed k_4 values resulted in a somewhat lower V_{ND} with smaller variability (k_4 = 0.011 min^{-1}, V_{ND} = 1.2, 22% COV; k_4 = 0.04 min^{-1}, V_{ND} = 0.9, 17% COV) (Fig. 3).

Next, we compared the impact of 2-TCM parameters, such as V_B (fixing to 5% or as a fit parameter), blood delay (no delay or as a fit parameter), and k_4 constraints (k_4 = 0.011 and 0.02 min^{-1}, $k_4 \geq 0.01$ min^{-1}, or as a fit parameter), on striatal specific binding values using DVR-1 derived from $V_{T,\ striatum}/V_{ND,\ cerebellum}$-1 (Fig. 4A). The results show that the data points were more scattered with unconstrained k_4, whereas a lower degree of dispersion was observed when $k_4 \geq 0.01$ min^{-1}. As k_4 negatively correlated to V_{ND} (Fig. 3), DVR-1 calculated with k_4 fixed to 0.02 min^{-1} was approximately 35% larger than DVR-1 calculated with k_4 fixed to 0.011 min^{-1} (k_4 = 0.02 min^{-1} 5.7 ± 1.4 vs. k_4 = 0.011 min^{-1} 4.2 ± 1.2). Other factors such as blood delay and V_B showed a small impact on DVR-1 estimates (Fig. 4A). Therefore, V_T and V_{ND} at baseline and under receptor saturation conditions were estimated by fitting V_B and blood delay to allow for variation in delay and V_B between animals and experiments, but with k_4 being constrained $\geq$ 0.01 min^{-1} to stabilize the fits. The results are presented in Figures 4B and 4C. V_T values were 5.8–7.4 in $A_{2A}R$-rich regions and 1.3–1.6 in reference regions at baseline.

Preladenant pretreatment significantly ($P < 0.001$) reduced the V_T in $A_{2A}R$-rich regions to about 1.1, which was comparable with V_T in reference regions (~1.0). However, the pretreatment with blockers also reduced the V_T in reference regions by 27%–33% (Fig. 4C), albeit the difference did not reach statistical significance. Because of the animal welfare issues, KW-6002 pretreatment was unable to achieve complete $A_{2A}R$ blockade (Fig. 4C). A dose of intravenous KW-6002 (1 mg/kg) resulted in adverse effects, and therefore higher doses were not tested. In addition to the cerebellum, we evaluated the cingulate, occipital cortex, and parietal cortex as reference regions to predict striatal BP_{ND}, because V_T values in these regions are comparatively low and stable (Fig. 4B).

BP_{ND} values obtained from the noninvasive SRTM with various reference regions as input were in agreement with DVR-1 in general (Figs. 4A and 5), with a positive bias of 20% ± 17% when k_4 was constrained to above 0.01 min^{-1}. Models with the cerebellum as the reference region displayed the highest BP_{ND} in $A_{2A}R$-rich regions, being approximately 5.3 (23% COV) in the putamen and 4.3 (25% COV) in the caudate. In comparison with the cerebellum, the parietal cortex as the reference region estimated slightly lower (8%) BP_{ND} with comparable variability (0%–1% difference, depending on brain regions) but higher test–retest reproducibility, showing a TRV value of 22% whereas 29% was calculated using the cerebellum as the reference region. Other reference regions estimated low BP_{ND} values with low test–retest reproducibility; therefore, these regions are less optimal reference regions to quantify tracer kinetics in the striatum. The between-subject variability for V_T and BP_{ND} was comparable (11%–30% COV). TRV was larger for V_T and DVR-1 calculated with the 2-TCM, 31%–43%, in comparison with 22%–29% TRV for BP_{ND} determined with the SRTM. Preladenant preinjection (1 mg/kg) reduced the BP_{ND} values in target

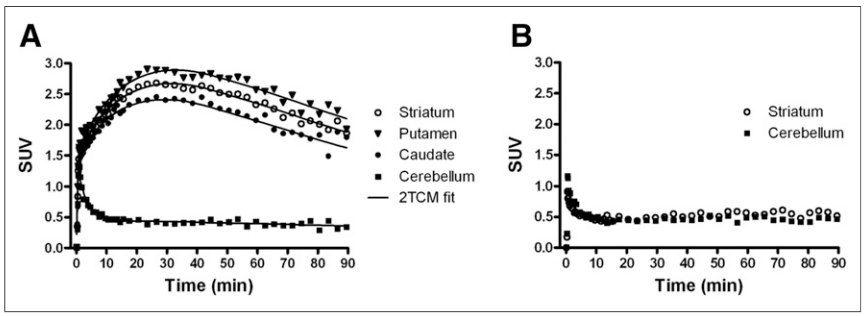

FIGURE 2. (A) Representative time–activity curves and 2-TCM fits of striatum, putamen, caudate, and cerebellum at baseline. (B) Time–activity curves of striatum and cerebellum after preladenant (1 mg/kg) pretreatment.

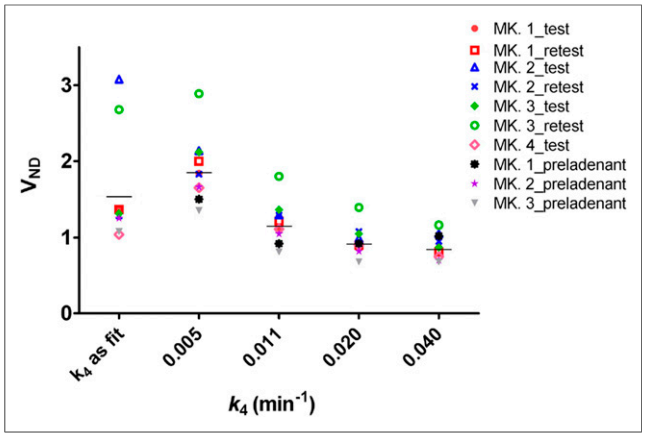

FIGURE 3. Effect of k_4 on V_{ND}. V_{ND} was obtained as V_T in cerebellum from 7 baseline scans and as V_T in striatum from 3 scans with preladenant preblocking. Horizontal lines represent mean of 10 scans. MK = monkey.

regions to about 0, indicating a complete blockade. Pretreatment with KW-6002 resulted in decreased tracer uptake in the striatum in all cases, with BP_{ND} values of 1.0 at 1 mg/kg ($n = 1$) and 2.0 ± 0.7 at 0.5 mg/kg ($n = 3$). In 1 case, no effect of 0.5 mg/kg of KW-6002 was observed, because the BP_{ND} in this animal was 7.4.

Furthermore, we investigated whether BP_{ND} was still robust with 61-min analysis by correlating DVR-1 and BP_{ND} obtained from 91-min scans with BP_{ND} obtained from the first 61-min analysis of the same scans (Fig. 6). Despite the positive bias of BP_{ND} related to DVR-1, a good correlation was found between the parameters, with a root mean square error value of 0.49 measured between data points and the line of Deming regression, which is about 69% of the smallest value ($BP_{ND} = 0.70$) and 6.8% of the largest value ($BP_{ND} = 7.1$). Moreover, there was no difference in BP_{ND} estimation between 91- and 61-min analysis, because the linear regression line (slope = 1.0, y-intercept = 0.17) was almost identical to the line of identity.

A_{2A}R Occupancy by Caffeine

Caffeine pretreatment reduced tracer uptake in A_{2A}R-rich regions in a dose-dependent manner (Fig. 7). Sixty-one- and 91-min analysis estimated comparable A_{2A}R occupancy, with a maximum difference of 1%, when the values were derived from BP_{ND} with the cerebellum as reference region. The BP_{ND} and A_{2A}R occupancy in the striatum after intravenous injection of 2.5, 5.0, and 10.0 mg/kg of caffeine were approximately 2.3, 1.5, and 0.8 and 64%, 74%, 81%, respectively. The parietal cortex as the reference region failed to estimate striatal BP_{ND} at the dose of 2.5 mg/kg.

DISCUSSION

We report the quantification of ^{11}C-preladenant uptake for the imaging of A_{2A}Rs in the conscious monkey brain. The tracer displayed a regional uptake that is in agreement with the known distribution of the receptor in the brain, with highest uptake in the putamen and caudate and lowest uptake in the cerebellum.

The tracer kinetics can be quantified with the 2-TCM in all brain regions. Regions devoid of receptor expression might be better fitted with 2-TCM than 1-TCM, because a small third (nonselective/metabolic) tissue compartment might exist in the brain, which is overwhelmed by the specific compartment in receptor-rich regions but not in receptor-poor regions. When the specific binding sites are blocked (Fig. 2B) or in regions without receptor expression, the specific binding compartment disappears and the influence of this small third tissue compartment on tracer kinetics emerges. The presence of a small (and slow) third tissue compartment resulted in difficulty in estimating k_4 in reference regions. In reference regions, the slow third tissue compartment caused time–activity curves to level off at later times, leading to very small k_4 values. Consequently, a 91-min acquisition might not be adequate and thus a longer scan might be necessary to have a better estimate of k_4 in reference regions. In our study, cerebellar k_4 could not be properly estimated in 2 of 7 baseline scans and in 1 scan with complete receptor blockade. Because the accuracy in V_{ND} estimate is essential to determine how much activity in

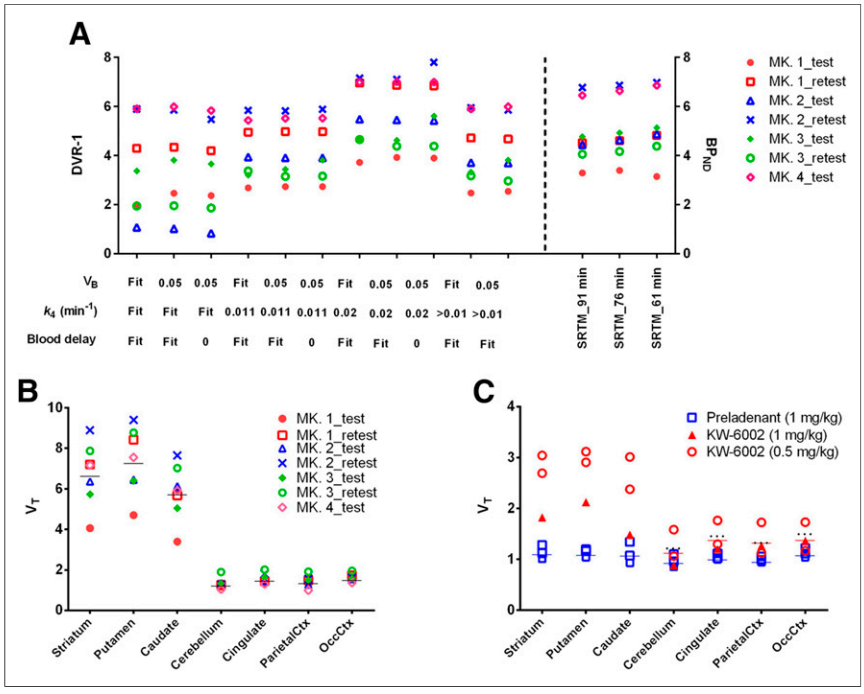

FIGURE 4. (A) Effect of blood volume, blood delay, and cerebellar k_4 on DVR-1 and a comparison in BP_{ND} between SRTM with different scan durations. Values were obtained using cerebellum as reference region. (B) V_T in striatum and reference regions at baseline. Horizontal lines represent mean of 7 baseline scans. (C) V_T in striatum and reference regions after blocker pretreatment. Solid horizontal lines represent mean of 3 preladenant preblocking scans (blue) and 3 KW-6002 preblocking scans (red, reference regions only). Dotted horizontal lines represent mean of 7 baseline scans (reference regions only). MK = monkey; OccCtx = occipital cortex; ParietalCtx = parietal cortex.

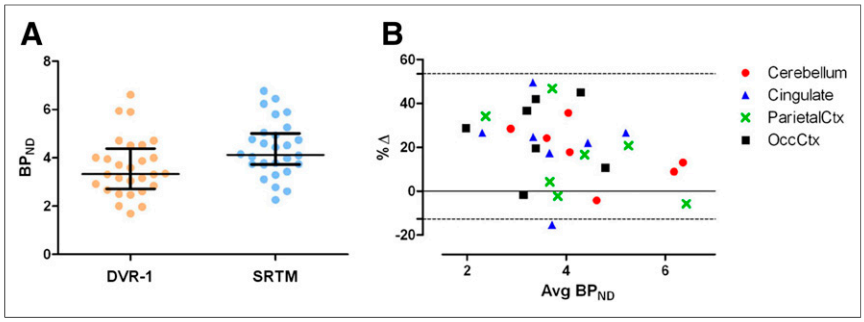

FIGURE 5. (A) Striatal BP_{ND} estimates from DVR-1 (2-TCM) and SRTM, using cerebellum, cingulate, parietal cortex, and occipital cortex as reference regions. Values were obtained from 7 baseline scans. Horizontal lines represent median with interquartile range. (B) Same datasets as in A but presented as Bland–Altman plot of difference (Δ) between BP_{ND} and DVR-1 against means of BP_{ND} and DVR-1. Area between dotted lines represents 95% confidence interval. $\Delta\ (\%) = 2 \times 100 \times (BP_{ND} - (\text{DVR-1}))/(BP_{ND} + (\text{DVR-1}))$. Avg = average; OccCtx = occipital cortex; ParietalCtx = parietal cortex.

V_T is due to specific binding, and V_{ND} appeared sensitive to k_4, we have studied the effect of fixing or constraining k_4 on V_{ND} in both the cerebellum and the striatum with complete receptor blockade. We found that a small k_4 resulted in high V_{ND} values. Therefore, we recommend using the plasma input 2-TCM with k_4 constrained above 0.01 min^{-1}, resulting in more comparable V_{ND} estimates across studies (Fig. 3).

With V_{ND} stabilized by restraining k_4, we further estimated the specific binding in target regions using DVR-1 and examined the agreement between DVR-1 and BP_{ND} obtained from the SRTM (Fig. 4A). The 2 measures correlated well with each other, with an average bias of +20% for BP_{ND}. However, BP_{ND} is favorable to DVR-1 in terms of smaller dispersion and TRV. Next, we investigated whether BP_{ND} was still robust with a 61-min acquisition. An excellent agreement was found in BP_{ND} between 61- and 91-min analysis. A good positive correlation was also observed between 61-min BP_{ND} and 91-min DVR-1 (Fig. 6), although the correlation became worse at small BP_{ND} (i.e., $BP_{ND} \leq 1.5$ [Fig. 6A]), because both methods lose the robustness of measuring specific binding in regions lacking specific binding sites. Taken together, our findings suggest that striatal BP_{ND} can be reliably quantified with a 61-min dynamic PET acquisition. A 61-min scan protocol was also adequate to study the $A_{2A}R$ occupancy by caffeine, because a high degree of consistency was observed across 61- and 91-min analysis (Fig. 7).

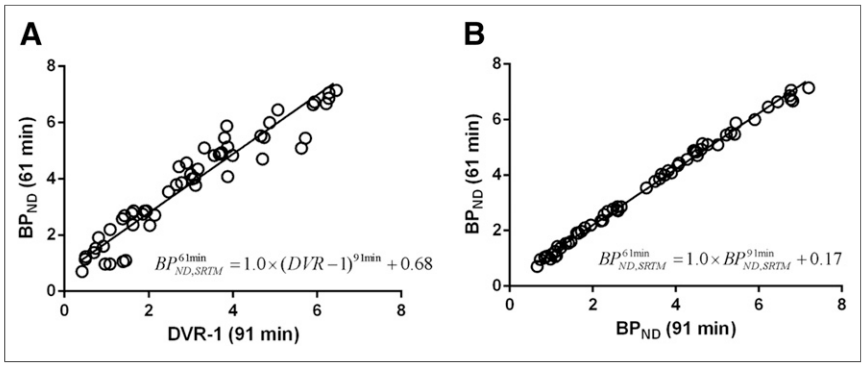

FIGURE 6. (A) Deming linear regression of BP_{ND} on DVR-1. (B) Deming linear regression of BP_{ND} obtained from 91- and 61-min analysis. BP_{ND} and DVR-1 were derived by reference to cerebellum.

Pretreatment with a blocker decreased the V_T values in the reference regions by approximately 30% (Fig. 4C, for clarity, caffeine data are not presented). A reduction in V_T in reference regions after blocker treatment was also found with ^{18}F-labeled preladenant (^{18}F-MNI-444) in a monkey study (*16*) but not in a rat study with ^{11}C-preladenant (*17*). In another rat study with ^{11}C-SCH442416 PET, using percentage injected dose per gram as the outcome parameter, tracer uptake in the cerebellum and cortex was also reduced after KW-6002 treatment (*18*). Some of the results may indicate the existence of specific binding to $A_{2A}R$ in reference regions (e.g., cerebellum). However, considering the low density of $A_{2A}R$ in extrastriatal regions (<10% density of $A_{2A}R$ in the striatum) (*19*) and the limited sensitivity of available PET tracers for $A_{2A}R$ ($BP_{ND} < 10$ in target regions), it is unlikely that these tracers are able to pick up the signal due to specific binding from the noise (background) in extrastriatal regions. We have observed a higher plasma parent activity concentration after pretreatment with a blocker than at baseline. Although the difference was not statistically significant, this might still contribute to a decrease in V_T in blocking experiments because the time–activity curves in reference regions at baseline and in blocking studies are similar. Moreover, the presence of the blocking agents might also influence the plasma free fraction, which is positively correlated to V_{ND} and V_T (*15*). The decrease in V_T in reference regions after blocker treatment might cause a bias in BP_{ND} calculations in receptor occupancy studies if such a decrease is mainly due to blocking of specific signal in these regions. Further studies are needed to find out whether such effect is species-specific and whether the reduction in V_T is actually significant (it is not significant in our case). Among all investigated reference regions, the cerebellum is favored over others in terms of low V_T and robustness of BP_{ND} estimation.

A potential pitfall in our study might be the nonnegligible impact of injected mass of preladenant on BP_{ND} and V_T, because a mass-dependent decrease in BP_{ND} was observed at baseline (Supplemental Fig. 3), due to variable specific activity of the tracer. Differences in specific activity between test and retest scans could account for the relatively high TRV (22%–29%) in this study, in comparison with our rat study (TRV, 6%), in which $A_{2A}R$ occupancy was always <5% due to coadministered preladenant with ^{11}C-preladenant (*17*). The masses of preladenant (3–10 nmol/kg) injected in this study could result in approximately 15%–30% of $A_{2A}R$ occupancy (*16*). When the true BP_{ND} at baseline was obtained by correcting the apparent BP_{ND} at baseline with 15%–30% self-occupancy by unlabeled preladenant, the TRV in BP_{ND} decreased to 14%–22% (Supplemental Fig. 4). Furthermore, the $A_{2A}R$ occupancy at caffeine doses of 2.5, 5, and 10 mg/kg became 70%, 72%,

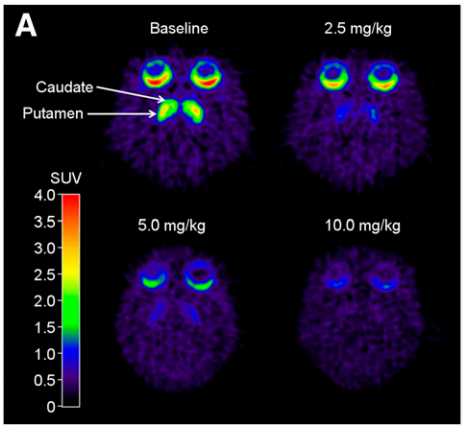

% occupancy

Target region	91 min			61 min		
	Caffeine dose (mg/kg)					
	2.5	5.0	10.0	2.5	5.0	10.0
Striatum	64	74	81	64	74	81
Putamen	64	72	79	64	73	79
Caudate	66	79	84	66	78	85

FIGURE 7. PET images of transverse view of monkey brain over 91-min scan (A) and corresponding time–activity curves in striatum (B) at baseline (open circle) and after intravenous injection of caffeine at 2.5 (triangle), 5.0 (cross), and 10.0 (closed circle) mg/kg (BP_{ND} of 6.9, 2.3, 1.5, and 0.8, respectively). Table shows estimated $A_{2A}R$ occupancy (%) in $A_{2A}R$-rich regions at corresponding caffeine doses based on 91- and 61-min analysis. BP_{ND} for occupancy calculation was obtained from SRTM with cerebellum as reference region. Occupancy = $\frac{BP_{ND,\ baseline} - BP_{ND,\ blocking}}{BP_{ND,\ baseline}} \times 100\%$.

and 81%, respectively, after correction for self-occupancy (*16,20*). Regardless of possible nonnegligible receptor occupancy by preladenant, our study demonstrated that ^{11}C-preladenant has suitable binding properties and pharmacokinetic profile, which warrants its translation to human studies. In human studies, issues regarding the injected mass dose of the tracer are less likely to occur, because humans have a 10- to 15-fold-higher body weight than the monkeys in this study and modern clinical PET cameras require a 2- to 3-fold-lower injected ^{11}C-preladenant dose for proper counting statistics than the animal scanner applied here.

CONCLUSION

^{11}C-preladenant showed a regional uptake in the conscious monkey brain that is in accordance with the known $A_{2A}R$ distribution, with high uptake in the striatum and low uptake in the cerebellum. The tracer kinetics in the striatum can be well described with the 2-TCM and SRTM. A 61-min dynamic acquisition is sufficient for adequate assessment of BP_{ND}, whereas a scan duration of more than 91 min might be necessary to have a robust estimation on k_4 in reference regions. Pretreatment with caffeine reduced the tracer uptake in $A_{2A}R$-rich regions in a dose-dependent manner, indicating that ^{11}C-preladenant PET is suitable to study $A_{2A}R$ occupancy with $A_{2A}R$-targeting molecules.

DISCLOSURE

No potential conflict of interest relevant to this article was reported.

ACKNOWLEDGMENT

We thank Michel Koole for suggestions on experimental design.

REFERENCES

1. El Yacoubi M, Costentin J, Vaugeois J-M. Adenosine A_{2A} receptors and depression. *Neurology.* 2003;61(11, suppl 6)S82–S87.
2. Glass M, Dragunow M, Faull RLM. The pattern of neurodegeneration in Huntington's disease: a comparative study of cannabinoid, dopamine, adenosine and $GABA_A$ receptor alterations in the human basal ganglia in Huntington's disease. *Neuroscience.* 2000;97:505–519.
3. Canas PM, Porciúncula LO, Cunha GMA, et al. Adenosine A_{2A} receptor blockade prevents synaptotoxicity and memory dysfunction caused by beta-amyloid peptides via p38 mitogen-activated protein kinase pathway. *J Neurosci.* 2009;29:14741–14751.
4. Schwarzschild MA, Agnati L, Fuxe K, Chen J-F, Morelli M. Targeting adenosine A_{2A} receptors in Parkinson's disease. *Trends Neurosci.* 2006;29:647–654.
5. Preti D, Baraldi PG, Moorman AR, Borea PA, Varani K. History and perspectives of A_{2A} adenosine receptor antagonists as potential therapeutic agents. *Med Res Rev.* 2015;35:790–848.
6. Ramlackhansingh AF, Bose SK, Ahmed I, Turkheimer FE, Pavese N, Brooks DJ. Adenosine 2A receptor availability in dyskinetic and nondyskinetic patients with Parkinson disease. *Neurology.* 2011;76:1811–1816.
7. Mishina M, Ishiwata K, Naganawa M, et al. Adenosine A_{2A} receptors measured with [^{11}C]TMSX pet in the striata of Parkinson's disease patients. *PLoS One.* 2011;6:e17338.
8. Rissanen E, Virta JR, Paavilainen T, et al. Adenosine A_{2A} receptors in secondary progressive multiple sclerosis: a [^{11}C]TMSX brain PET study. *J Cereb Blood Flow Metab.* 2013;33:1394–1401.
9. Mishina M, Ishiwata K, Kimura Y, et al. Evaluation of distribution of adenosine A_{2A} receptors in normal human brain measured with [^{11}C]TMSX PET. *Synapse.* 2007;61:778–784.
10. Zhou X, Khanapur S, Huizing AP, et al. Synthesis and preclinical evaluation of 2-(2-furanyl)-7-[2-[4-[4-(2-[^{11}C]methoxyethoxy)phenyl]-1-piperazinyl]ethyl] 7H-pyrazolo[4,3-e][1,2,4]triazolo[1,5-c]pyrimidine-5-amine ([^{11}C]preladenant) as a PET tracer for the imaging of cerebral adenosine A_{2A} receptor. *J Med Chem.* 2014;57:9204–9210.
11. Neustadt BR, Hao J, Lindo N, et al. Potent, selective, and orally active adenosine A_{2A} receptor antagonists: arylpiperazine derivatives of pyrazolo[4,3-e]-1,2,4-triazolo[1,5-c]pyrimidines. *Bioorg Med Chem Lett.* 2007;17:1376–1380.
12. Fredholm BB. Astra Award Lecture. Adenosine, adenosine receptors and the actions of caffeine. *Pharmacol Toxicol.* 1995;76:93–101.
13. Watanabe M, Okada H, Shimizu K, et al. A high resolution animal PET scanner using compact PS-PMT detectors. *IEEE Trans Nucl Sci.* 1997;44:1330–1334.
14. Jones EG, Stone JM, Karten HJ. High-resolution digital brain atlases: a Hubble telescope for the brain. *Ann N Y Acad Sci.* 2011;1225(suppl 1):E147–E159.
15. Innis RB, Cunningham VJ, Delforge J, et al. Consensus nomenclature for in vivo imaging of reversibly binding radioligands. *J Cereb Blood Flow Metab.* 2007;27:1533–1539.
16. Barret O, Hannestad J, Alagille D, et al. Adenosine 2A receptor occupancy by tozadenant and preladenant in rhesus monkeys. *J Nucl Med.* 2014;55:1712–1718.
17. Zhou X, Khanapur S, de Jong JR, et al. In vivo evaluation of [^{11}C]preladenant positron emission tomography for quantification of adenosine A_{2A} receptors in the rat brain. *J Cereb Blood Flow Metab.* 2017;37:577–589.
18. Moresco RM, Todde S, Belloli S, et al. In vivo imaging of adenosine A_{2A} receptors in rat and primate brain using [^{11}C]SCH442416. *Eur J Nucl Med Mol Imaging.* 2005;32:405–413.
19. Lopes LV, Halldner L, Rebola N, et al. Binding of the prototypical adenosine A_{2A} receptor agonist CGS 21680 to the cerebral cortex of adenosine A_1 and A_{2A} receptor knockout mice. *Br J Pharmacol.* 2004;141:1006–1014.
20. Tavares AAS, Caillé F, Barret O, et al. In vivo evaluation of ^{18}F-MNI698: an ^{18}F-labeled radiotracer for imaging of serotonin 4 receptors in brain. *J Nucl Med.* 2014;55:858–864.